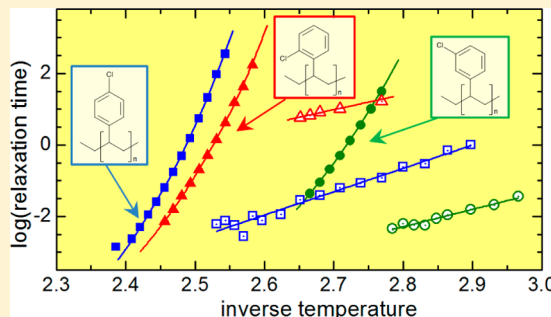


Effect of Regioisomerism on the Local Dynamics of Polychlorostyrene

R. Casalini* and C. M. Roland

Chemistry Division, Naval Research Laboratory, Code 6120, Washington, D.C. 20375-5342, United States

ABSTRACT: Relaxation properties of three isomers of atactic polychlorostyrene, having the chlorine atom in the ortho, meta, and para positions (P2CS, P3CS, and P4CS, respectively), were measured by mechanical and dielectric spectroscopies and modulated scanning calorimetry. For the α relaxation, the more spatially extended pendant group in P4CS gives rise to steric constraints on the segmental dynamics that cause both the temperature dependence of its relaxation time (i.e., the fragility) and the number of dynamically correlated segments to be largest. For the secondary β -relaxation in P4CS, the chlorophenyl moiety can rotate (spin) without involving the backbone; that is, the motion involves internal degrees of freedom. Consequently, this secondary relaxation is high in frequency and has a weak relaxation strength, especially as measured dielectrically. On the other hand, the pendant group in P2CS cannot reorient without adjustments in position of the backbone segments, causing its β relaxation strength measured mechanically to be the largest. Since all atoms in the repeat unit for P2CS participate in the secondary dynamics, it is classified as a Johari–Goldstein (JG) process. As generally found for JG relaxations, the behavior of the β relaxation in P2CS is affected by the density changes accompanying physical aging.



INTRODUCTION

Although chain motions and segmental relaxation are of primary interest in unraveling structure–property relations in polymers, the secondary dynamics are also important, through both their potential influence on physical properties^{1–6} and their putative connection to the glass transition.^{7,8} Polymers can exhibit myriad secondary motions, particularly when polyatomic pendant groups are present. In their classic text, McCrum, Read, and Williams⁹ described the different dynamics that underlie polymer secondary relaxations, including pendant group reorientations and (largely discredited¹⁰) crankshaft motions within the chain backbone. Unique among secondary relaxations is the Johari–Goldstein (JG) relaxation, which is universal in glass-forming substances.^{11–13} The JG process involves reorientation of the entire molecule or repeat unit in a polymer, at frequencies intermediate between the slow primary α relaxation (segmental dynamics) and any secondary relaxations involving intramolecular degrees of freedom. Much attention has focused on the JG relaxation to investigate any role in structural relaxation. The properties of the JG relaxation include^{14–16} (i) merging with the α process at high temperatures, (ii) changing behavior when the temperature of the material goes through the glass transition temperature T_g , (iii) a separation in frequency from the α relaxation that is correlated with the breadth of the α dispersion, and (iv) sensitivity to density changes, brought about by either pressure or physical aging. Note some non-JG processes display at least some of these same properties.^{17–19}

The seminal papers reporting JG motion in several molecular liquids included data on chlorobenzene.²⁰ The experiments on

this rigid molecule confirmed the existence of relaxation even in molecules in the glassy state that do not have internal modes of motion. In the present work we study dielectric relaxation of chlorobenzene tethered to a polyethylene backbone, the structure corresponding to one of the three positional isomers of atactic polychlorostyrene. The dipole moment of the backbone is negligible compared to that of the chlorostyrene, so the dielectric measurements probe the dynamics of the polar side group. If rotation of the pendant group entails motion of the chain segment, this probe senses the α and JG relaxations. However, if the benzene ring can orient independently of the main chain, the motion corresponds to non-JG dynamics. In the present work we find that the nature of the secondary relaxations, including both their amplitude and rate, in regioisomers of poly(4-chlorostyrene) depends on the position of the chlorine atom on the phenyl ring. For P4CS the pendant group reorientation proceeds independently, without involving motion of the polymer backbone. In contrast, angular displacement of the 2-chlorostyrene is coupled to rotation about the main chain bonds, so that the changes in polarization are manifested as a JG process. The constraints on the pendant group in P3CS are intermediate, and whether its secondary relaxation is a JG process cannot be determined from the available data.

The number of dynamically correlated segments were estimated for the polymers both from the dielectric data and

Received: April 23, 2014

Revised: May 30, 2014

Published: June 5, 2014

using modulated DSC; the results were trendwise equivalent. We also measured mechanical spectroscopy on the polychlorostyrenes. Although the dynamics underlying the mechanical loss are essentially those governing the dielectric response, the mechanical relaxation strength does not depend on the dipole moment of the chlorobenzene ring, but rather on the magnitude of local strain induced by motion of this group. The results of the present study show how subtle changes in chemical structure can effect large changes in the dynamic properties of polymer glasses.

EXPERIMENTAL SECTION

The polymers studied herein were poly(2-chlorostyrene) (P2CS), poly(3-chlorostyrene) (P3CS), and poly(4-chlorostyrene) (P4CS), all atactic, with the respective repeat units shown in Figure 1. The

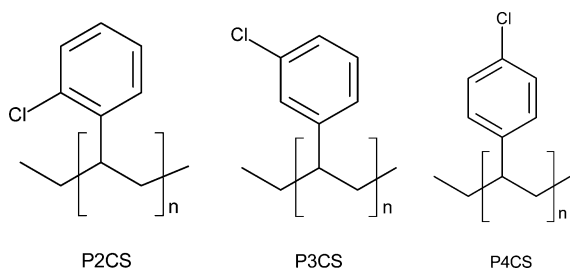


Figure 1. Molecular structure of three polychlorostyrene regioisomers.

materials were obtained from Scientific Polymer Products and used as received. The molecular weights determined from light scattering were all in excess of 80 kg/mol, ensuring asymptotic behavior of the segmental dynamics.

Differential scanning calorimetry was conducted with a TA Q100, using a scanning rate of 10 K/min. For modulated differential scanning calorimetry (MDSC) the rate was 0.5 K/min, with four modulation periods (120, 90, 60, and 40 s) and a modulation amplitude of 1 K.

Rheological measurements employed an Anton Parr MCR 502, using a parallel plate geometry (diameter = 8 mm). Samples were molded under vacuum and maintained in a nitrogen atmosphere during the measurements. Broadband dielectric spectra were measured with a Novocontrol impedance analyzer. The samples were pressed above T_g between two parallel plates (diameter = 16 mm) separated by 100 μm Teflon spacers. During the experiment the sample was under vacuum, with temperature controlled with a closed cycle helium cryostat.

RESULTS

Mechanical Spectroscopy. Representative dynamic loss modulus spectra are shown in Figure 2 for P2CS. There is an intense peak corresponding to segmental relaxation at temperatures in the range from ca. 389 to 405 K. Defining a mechanical glass transition as the temperature at which $\tau_\alpha = 100$ s yields the values listed in Table 1 for P2CS and the other two isomers. The differences in T_g are consistent with those measured by calorimetry (Table 1), although the latter are several degrees higher. The segmental loss peaks for the three isomers are compared in Figure 3 for temperatures at which the τ_α are the same (≈ 3 s). The dispersion for P2CS is substantially broader, with the peak described by the Kohlrausch function^{21,22}

$$G''(\omega) = \Delta G_\alpha L_{i\omega} \left[-\frac{d\varphi_\alpha(t, \tau_\alpha)}{dt} \right]$$

with $\varphi(t, \tau_\alpha) = \exp[-(t/\tau_\alpha)^{\beta_{\text{KWW}}}]$ (1)

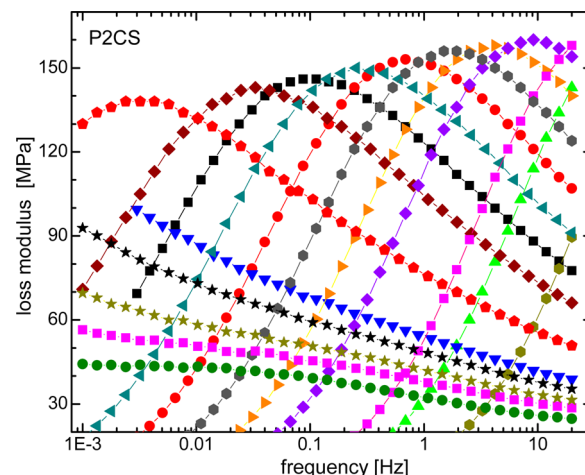


Figure 2. Mechanical loss spectra of P2CS at various temperatures. From left to right T ($^{\circ}\text{C}$) = 142, 138, 136, 132, 130, 128, 126, 124, 122, 120, 116, 110, 108, 104, 100, and 92.

Table 1. Glass Transition Temperatures

	T_g [K]		
	DSC (midpoint)	mechanical ($\tau_\alpha = 100$ s)	dielectric ($\tau_\alpha = 100$ s)
P2CS	397	388	393
P3CS	363	359	361
P4CS	401	395	398

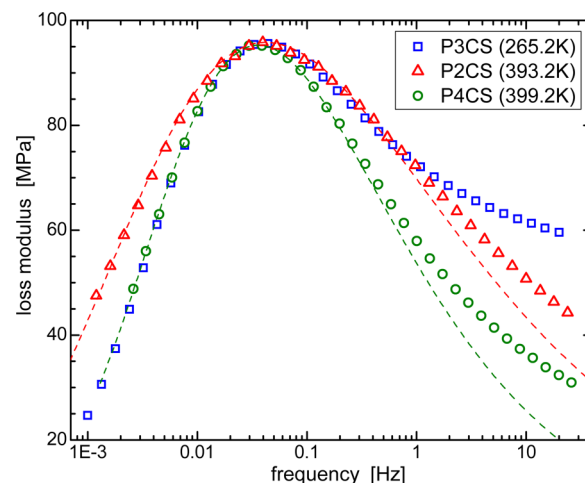


Figure 3. Comparison of mechanical loss peaks of the polychlorostyrene. Dotted lines are fits of the KWW relaxation function (eq 1).

where $L_{i\omega}$ indicates the Laplace transform. Fitting the α peak for P2CS yields $\beta_{\text{KWW}} = 0.29$, whereas for P4CS $\beta_{\text{KWW}} = 0.39$. The loss peak for the P3CS is narrow on the low frequency side but broadens significantly toward higher frequencies due to a partially overlapping secondary peak. This can be seen more clearly in Figure 4, showing the loss modulus for P3CS at temperatures through T_g . At the highest temperature (within 0.1 K of the calorimetric T_g) the segmental relaxation time determined from the peak frequency is 11 s. At all lower temperatures in Figure 4, the maximum of the segmental peak falls at frequencies lower than experimentally measured, with the weak β -relaxation emerging as a distinct peak in the glassy state. The other two polymers show similar behavior. The β -

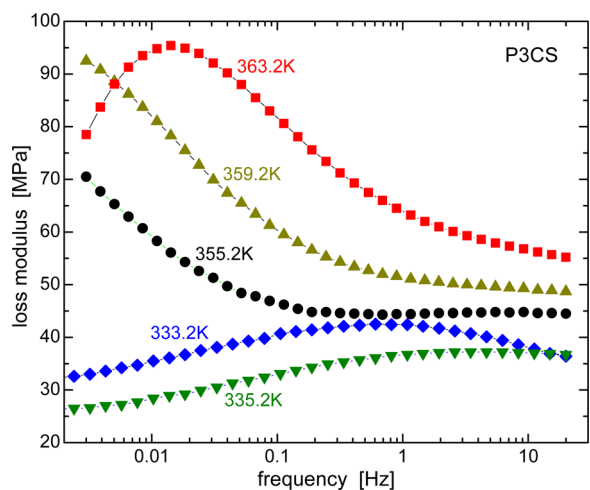


Figure 4. Mechanical loss spectra of P3CS in the vicinity of the glass transition. Above T_g the spectra are dominated by the α relaxation, with the secondary β peak emerging at lower temperatures.

peak is much broader than the α -relaxation, with the Cole–Cole relaxation function²¹ used to fit the former

$$G''(\omega) = \frac{\Delta G_\beta}{1 + (i\omega\tau_\beta)^{1-\alpha_{cc}}} \quad (2)$$

Dielectric Spectroscopy. Representative dielectric loss peaks are shown in Figure 5 for the three isomers, superposed

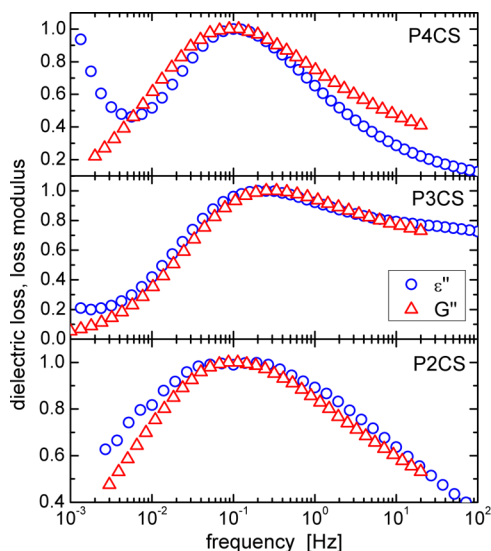


Figure 5. Comparison of the dielectric and mechanical loss spectra for the three isomers.

on the corresponding mechanical loss peaks. The shapes are comparable, recognizing there is an influence from the secondary relaxation and ionic conductivity. Similar to the mechanical spectra, for all three isomers a broad β relaxation is apparent below T_g . The analysis of the dielectric spectra was done similarly to the mechanical results, using a linear superposition of a KWW function for the α relaxation and a CC function for the β process

$$\begin{aligned} \varepsilon^*(\omega) = \Delta\varepsilon_\alpha L_{i\omega} \left[-\frac{d\varphi_\alpha(t, \tau_\alpha)}{dt} \right] + \frac{\Delta\varepsilon_\beta}{1 + (i\omega\tau_\beta)^{1-\alpha_{cc}}} \\ + \frac{\sigma_{dc}}{\varepsilon_0(i\omega)^n} + \varepsilon_\infty \end{aligned} \quad (3)$$

where σ_{dc} is the dc conductivity due to mobile ions.

The relaxation strength of the two processes is strongly dependent on the structure of the repeat unit (Table 2). P3CS

Table 2. Kohlrausch Exponents and Relaxation Strength

	β -relaxation strength (T_g^α)		α -relaxation strength (T_g)		$\beta_{KWW}(T_g)$	
	mech	diel	mech	diel	mech	diel
P2CS	580	0.19	870	0.26	0.25 ± 0.3^b	0.26 ± 0.2^b
P3CS	320	4.8	500	2.9	0.34 ± 0.3	0.47 ± 0.2
P4CS	160	0.06	570	0.94	0.37 ± 0.2	0.47 ± 0.2

^aExtrapolated from lower temperatures. ^bFit to convoluted α and β peaks.

has the largest dielectric strength, while P4CS has the smallest $\Delta\varepsilon_\beta$ and P2CS the smallest $\Delta\varepsilon_\alpha$. If $\Delta\varepsilon_\alpha$ were proportional to the component of the dipole moment perpendicular to the chain, it would be largest for P4CS and comparable for P2CS and P3CS. This is not the case, however, because the dipole in P4CS reorients by rotation about a bond tethering it to the backbone, and such motion does not change the transverse dipole moment. In contrast, the reorientation of the chlorostyrene moiety in the other isomers effects a significant change in the dipole moment. For P2CS the proximity of the chlorobenzene group to the chain causes steric hindrance that restricts rotation around the C–C bond. Note that the mechanical relaxation strengths (Table 2) provide a direct indication of this coupling, with the values for the three polymers falling in order according to the relative degree of constraint from backbone on motion of the side group. These interactions are reflected in the breadths of the α peaks in the dielectric and mechanical spectra (Table 2). Since the β process in P4CS is noncooperative, we expect that there should be another secondary relaxation, the JG process, between the α and β peaks. However, none is apparent in Figure 6, suggesting it is too weak or unresolved.

From the coupling of the side group and backbone dynamics in P2CS, the secondary relaxation should be sensitive to volume. To test this prediction, dielectric measurements were made as a function of time during physical aging at 13 K below T_g . As seen in Figure 7, there is a systematic decrease in the intensity of the dielectric loss (shown at a fixed frequency of 1 Hz in the figure). This change in amplitude occurs without any change in the shape of the β peak. The kinetics of the aging-induced changes can be described with a stretched exponential function^{23,24}

$$\varepsilon''(\bar{f}, t_{\text{aging}}) = a \exp \left[-\left(\frac{t_{\text{aging}}}{\tau_{\text{age}}} \right)^{\beta_K} \right] + b \quad (4)$$

where b is the ε'' long time (equilibrium) value and a is a constant. The fit to the data in Figure 7 yields for the aging time constant, $\tau_{\text{age}} = (2.1 \pm 0.3) \times 10^4$ s, a result independent of the frequency used for the analysis. As shown in earlier work,^{23,25} τ_{age} reflects the value of τ_α in the glassy state, and the

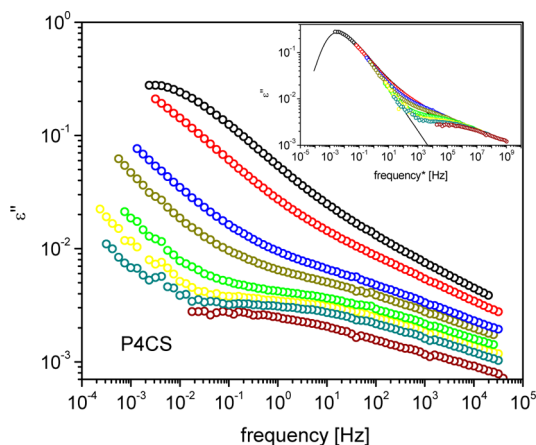


Figure 6. Dielectric loss spectra of P4CS in the vicinity of T_g . Temperatures (K) from right to left = 399.7, 386.5, 390.3, 387.5, 382.1, 376.2, 370.1, and 349.6. The inset shows the data after shifting the spectra for lower temperatures to superpose on the high-frequency flank of the α peak at 399.7 K. Solid line represents eq 1 with $\beta_{\text{KWW}} = 0.47$.

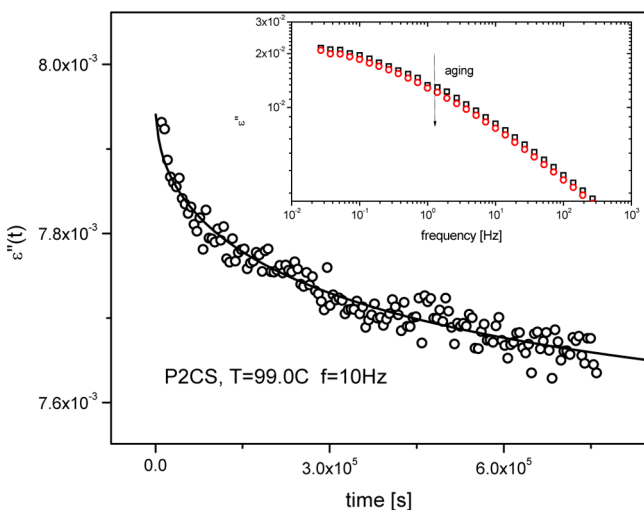


Figure 7. Physical aging of the secondary relaxation in P2CS. Main figure shows the time dependence of dielectric loss intensity at a fixed frequency; solid line is fit of eq 4 with $\tau_{\text{age}} = (2.1 \pm 0.3) \times 10^4$ s. Inset shows the spectra measured at the beginning and end of the aging experiment.

aging time determined herein for P2CS is consistent with the τ_α measured directly above T_g (Figure 8).

Relaxation Map. In Figure 8 the segmental and secondary relaxation times for the three isomers measured by the two spectroscopies are plotted versus reciprocal temperature. The τ_α all conform to the Vogel–Fulcher (VF) equation for $T > T_g$. Segmental relaxation times are also shown for P4CS in the glassy state; these were estimated by fitting the spectra on the high frequency side, with the assumption that β_{KWW} and $\Delta\epsilon_\alpha$ are constant and equal to their values at T_g . The reduction in sensitivity to temperature below T_g seen in Figure 8 is common,^{23,25–27} a result of the weaker volume changes (smaller thermal expansion coefficient) for the glass.

Comparing apparent activation energies at T_g , P4CS is the most fragile (largest steepness index). The inference is that its larger cross-section sweeps out more volume, causing stronger intermolecular cooperativity for the motion. However, this is

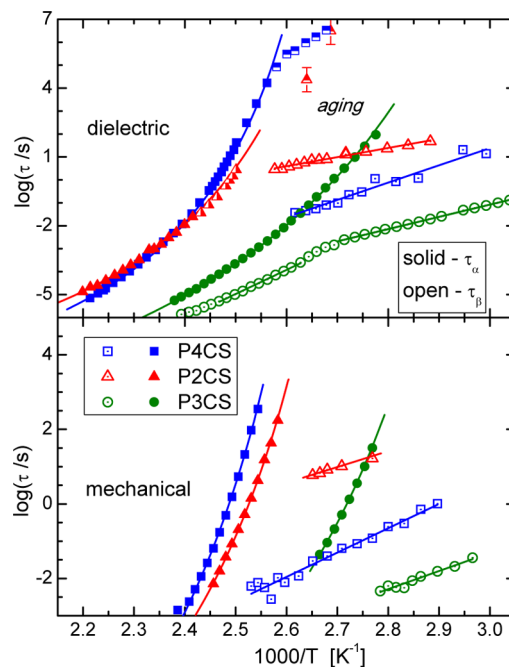


Figure 8. Relaxation map for the dielectric and mechanical data. The half-filled triangles for τ_α of P2CS were obtained by fitting the overlapping α and β dielectric peaks with a single relaxation function.

not associated with a broader dispersion; the loss peak for P4CS is the narrowest of the three isomers. This disconnect between temperature sensitivity and peak breadth is unusual.²⁸ An alternative point of view is that the position of the Cl in P4CS limits the number of available configurations, resulting in a narrower distribution of relaxation times and hence a narrower α peak. In an entropy interpretation of the glass transition,^{29–32} the narrower spectra for P4CS are consistent with a smaller combination of motions being necessary to allow relaxation. In the case of P2CS the strong interaction between the side group and the backbone constrains the secondary dynamics, giving rise to smaller differences between τ_β and τ_α ; this interaction can also be used to rationalize its fragility.^{22,33}

All τ_β in the glassy state show Arrhenius behavior, with the activation energies listed in Table 3; mechanical and dielectric

Table 3. Temperature Dependences

	E_β [kJ/mol]		m		MDSC
	mech	diel	mech	diel	
P2CS	81 ± 10	76 ± 3	118 ± 12	91 ± 9	91 ± 9
P3CS	93 ± 7	102 ± 2/ 202 ± 2 ^a	100 ± 10	80 ± 4	85 ± 3
P4CS	122 ± 6	144 ± 9	127 ± 13	110 ± 7	112 ± 4

^aHigher E_β for $T > T_g$.

results are in good agreement. For P2CS the τ_β is more than 2 decades closer to τ_α than for the other polymers, a consequence of the coupling of the side group and backbone motions. For P3CS and P4CS, the separation in time scale between the α and β processes is about the same, ca. 3 decades. For P3CS, the only sample for which measurements could be obtained close to T_g , the dielectric relaxation times show a change in activation energy around $\tau_\alpha \approx 100$ s. This behavior has been seen previously in JG relaxations in glass-forming liquids³⁴ and taken to suggest that the JG secondary relaxation “senses” structural

relaxation. However, similar behavior was observed for some non-JG secondary relaxations as well.¹⁸ For P4CS the activation energy for the secondary relaxation is surprisingly large, considering the facile motion underlying it. An empirical correlation has been deduced between the JG activation energy and the glass transition temperature, $E_\beta \approx 24RT_g$.^{35,36} P2CS conforms well to this relation: $E_\beta/RT_g = 23.3 \pm 1$ and 25 ± 3 for the dielectric and mechanical data, respectively. However, for P4CS, $E_\beta/RT_g = 43 \pm 3$ (dielectric) and 36 ± 3 (mechanical), supporting our identification of the β relaxation as a non-JG process. For P3CS the values are 33.3 ± 1 (dielectric) and 31 ± 2 (mechanical), suggesting an intermediate character for its secondary motion.

MDSC Measurements. In Figure 9 are shown the real, c_p' , and imaginary, c_p'' , components of the heat capacity for the three

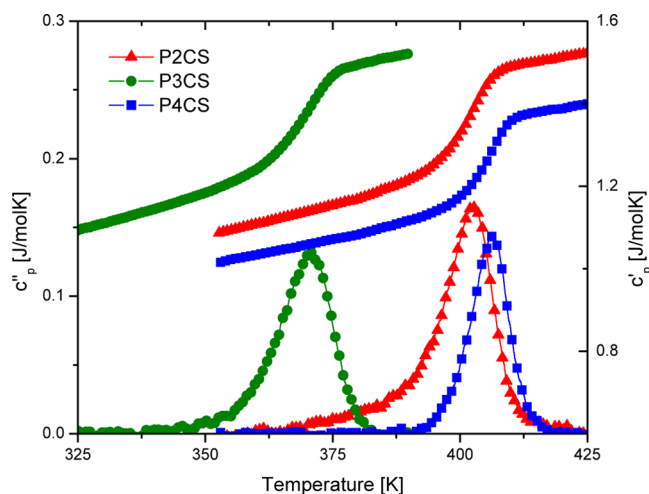


Figure 9. Real and imaginary components of the heat capacity for a 40 s modulation period.

polymers, measured with a modulation period of $T_m = 40$ s. The heat capacities were calculated after correcting for the change in heat capacity at the glass transition.^{37,38} The breadth (hwhm) of the c_p'' peaks, δT , was determined by fitting a Gaussian function to the data. The values of the temperature of the maximum and of δT are reported in Table 4 for a modulation period of 120 s. Defining a relaxation time $\hat{\tau}(T) = (T_m(T))/2\pi$, where $T_m(T)$ is the modulation period for which the maximum in c_p'' is at temperature T , we obtained the $\hat{\tau}(T)$ in Figure 10 (half-filled symbols); also included for comparison are the segmental relaxation times from the mechanical and dielectric experiments. For all three polymers, $\hat{\tau}(T)$ is significantly larger than τ_ω , consistent with the higher calorimetric T_g . The steepness indices from the MDSC data (Table 3) are consistent with the fragilities, again P4CS having the greatest T sensitivity.

The breadth of the peak in isochronal measurements is determined both by the breadth of the peak in isothermal

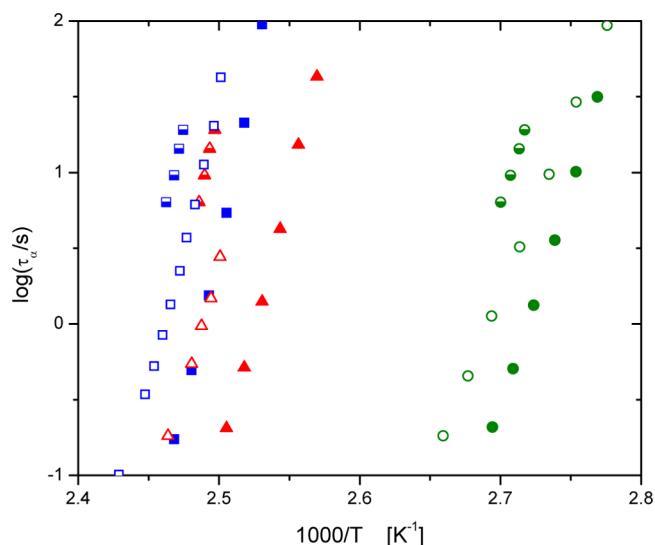


Figure 10. Relaxation map including the MDSC data. Square are P4CS, triangles P2CS, and circles P3CS. Solid symbol = dielectric; open symbols = mechanical; half-filled symbols = MDSC.

spectra (i.e., β_{KWW}) and by the temperature dependence of the relaxation time. The relevant expression is³⁹

$$\delta T \approx \frac{-1.07T}{\beta_{\text{KWW}}} \left(\frac{\partial \ln \tau_\alpha}{\partial \ln T} \right)^{-1} = \frac{1.07T}{\beta_{\text{KWW}} \ln(10)m} \quad (5)$$

Using this equation, we calculate from the MDSC measurements β_{KWW} that are significantly larger for P2CS. This may reflect the contribution of the secondary relaxation to the mechanical and dielectric spectra, whereas its absence in the MDSC measurements makes the spectra narrower.

Dynamic Heterogeneity. The dynamics of supercooled liquids is spatially heterogeneous, with an increasing dynamic correlation length with decreasing temperature or increasing density. A number of methods have been proposed to quantify the number of correlating units (atoms, molecules, or chain segments) from experimental data. An equation due to Donth⁴⁰ gives this number as

$$N_c = \frac{RT^2}{m_0(\delta T)^2} \Delta(c_p^{-1}) \quad (6)$$

where m_0 is the molecular weight of the relaxing unit, and δT can be determined from the c_p'' as discussed above. Taking $m_0 = 138.49$ (molecular weight of the repeat unit), we calculate for $\hat{\tau} = 14$ s values of N_c in the range from 58 for P3CS to 120 for P4CS (Table 4).

More recently Berthier et al.^{41,42} derived the equation

$$N_c = \frac{R}{\Delta c_p} T^2 \left\{ \max_t \chi_T(t) \right\}^2 \quad (7)$$

Table 4. MDSC for $\hat{\tau} = 14$ s

	2δ [K]	T [K]	N_c		Δc_p^{-1} [J/(K mol)]	c_p^{liquid} [J/(K mol)]	c_p^{glass} [J/(K mol)]	Δc_p [J/(K mol)]	β_{KWW}
			eq 8	eq 6					
P2CS	8.0	401	83	407	0.148	1.49	1.26	0.23	0.50 ± 0.04
P3CS	8.6	404.5	58	299	0.131	1.46	1.26	0.20	0.45 ± 0.02
P4CS	6.7	368.5	120	621	0.136	1.51	1.29	0.22	0.50 ± 0.02

where χ_T is the time derivative of the relevant correlation function. For a stretched exponential form (eq 3), eq 7 reduces to⁴³

$$N_c = \frac{R}{\Delta c_p m_0} \left(\frac{\beta_{\text{KWW}}}{e} \right)^2 \left(\frac{\partial \ln \tau_\alpha}{\partial \ln T} \right)^2 \quad (8)$$

where e is Euler's number. N_c from eq 8 differs from eq 6 by the factor $6.45 \Delta c_p \Delta(c_p^{-1})$.⁴⁴ The values calculated using eq 6 from the MDSC measurements (Table 4) are ~ 5 times higher than those from eq 8 but have the same trend with chemical structure. (Note that both eqs 6 and 8 are only approximate.) It is tempting to ascribe the difference in correlation lengths for the three polymers to aspects of their respective chemical structures; however, the cooperative dynamics in these dense, interacting materials are too complex for any facile relationship to be deduced.

CONCLUSIONS

The simple liquid chlorobenzene is a classic example of a material exhibiting a Johari–Goldstein relaxation. When attached to a polymer chain, this motion involves the repeat unit of the chain backbone only if there are steric interferences sufficient to couple the motion of the side group. This is the case for P2CS, and its secondary relaxation is a JG process. Consequently, the mechanical relaxation strength for the secondary relaxation in P2CS is large, the activation energy has the expected value, and the τ_β are sensitive to volume changes, as effected, for example, by physical aging. P4CS represents the opposite case. The phenyl group is free to rotate without involving the main chain segments, and thus the prominent secondary peak is not a JG process. The secondary relaxation of P4CS falls at higher frequencies and, since the spinning motion does not alter the dipole moment, has a low dielectric strength. The activation energy for the secondary relaxation in P4CS is much larger than expected from an empirical correlation for JG processes. P3CS is an intermediate case, the side group experiencing steric constraints that are weaker than those for P2CS and the β activation energy deviating from the correlation. A definitive assignment of its secondary relaxation cannot be made; molecule dynamics simulations would be useful in this regard.¹⁵

Properties of the local segmental dynamics (α relaxation) were also measured for the materials herein. P4CS has the most spatially extended pendant group and the largest fragility; this is consistent with larger local configurational adjustments being necessary to accommodate the segmental motion. This isomer also has the largest N_c . There is no correspondence between the breadth of the α dispersions and the fragility, possible due to the contribution to the former of an overlapping secondary relaxation.

AUTHOR INFORMATION

Corresponding Author

*E-mail riccardo.casalini@nrl.navy.mil (R.C.).

Notes

The authors declare no competing financial interest.

ACKNOWLEDGMENTS

This work was supported by the Office of Naval Research.

REFERENCES

- (1) Chen, L. P.; Yee, A. F.; Moskala, E. J. *Macromolecules* **1999**, *32*, 5944.
- (2) Monnerie, L.; Laupretre, F.; Halary, J. L. *Adv. Polym. Sci.* **2005**, *35*, 187.
- (3) Monnerie, L.; Halary, J. L.; Kausch, H. H. *Adv. Polym. Sci.* **2005**, *187*, 215.
- (4) Cicerone, M. T.; Douglas, J. F. *Soft Matter* **2012**, *8*, 2983.
- (5) Bhattacharya, S.; Suryanarayanan, R. J. *Pharm. Sci.* **2009**, *98*, 2935.
- (6) Wojnarowska, Z.; Roland, C. M.; Kolodziejczyk, K.; Swiety-Pospiech, A.; Grzybowska, K.; Paluch, M. *J. Phys. Chem. Lett.* **2012**, *3*, 1238–1241.
- (7) Ngai, K. L. *J. Chem. Phys.* **1998**, *109*, 6982.
- (8) Fragiadakis, D.; Roland, C. M. *Phys. Rev. E* **2012**, *86*, 020501(R).
- (9) McCrum, N. G.; Read, B. E.; Williams, G. *Anelastic and Dielectric Effects in Polymeric Solids*; John Wiley and Sons: New York, 1967.
- (10) Liao, T.-P.; Morawetz, H. *Macromolecules* **1980**, *13*, 1228–1233.
- (11) Pathmanathan, K.; Johari, G. P. *J. Polym. Sci., Part B: Polym. Phys.* **1987**, *25*, 379.
- (12) Jarosz, G.; Mierzwa, M.; Ziolo, J.; Paluch, M.; Shirota, H.; Ngai, K. L. *J. Phys. Chem. B* **2011**, *115*, 12709.
- (13) Yu, H.-B.; Wang, W.-H.; Samwer, K. *Mater. Today* **2013**, *16*, 183.
- (14) Ngai, K. L.; Paluch, M. *J. Chem. Phys.* **2004**, *120*, 857.
- (15) Fragiadakis, D.; Roland, C. M. *Phys. Rev. E* **2013**, *88*, 042307; **2014**, *89*, 052304.
- (16) Casalini, R.; Roland, C. M. *Phys. Rev. Lett.* **2003**, *91*, 015702.
- (17) Capaccioli, S.; Prevosto, D.; Lucchesi, M.; Rolla, P. A.; Casalini, R.; Ngai, K. L. *J. Non-Cryst. Solids* **2005**, *351*, 2643–2651.
- (18) Casalini, R.; Fioretto, D.; Livi, A.; Lucchesi, M.; Rolla, P. A. *Phys. Rev. B* **1997**, *56*, 3016–3021.
- (19) Santucci, S. C.; Corezzi, S.; Fioretto, D.; Capaccioli, S.; Casalini, R.; Lucchesi, M.; Presto, S.; Rolla, P. A. *IEEE Trans. Dielectr. Electr. Insul.* **2001**, *8*, 373–376.
- (20) Johari, G. P.; Goldstein, M. *J. Phys. Chem.* **1970**, *74*, 2034; *J. Chem. Phys.* **1970**, *53*, 2372.
- (21) Kremer, F.; Schonhals, A., Eds.; *Broadband Dielectric Spectroscopy*; Springer: Berlin, 2003.
- (22) Roland, C. M. *Viscoelastic Behavior of Rubbery Materials*; Oxford University Press: New York, 2011.
- (23) Casalini, R.; Roland, C. M. *Phys. Rev. Lett.* **2009**, *102*, 035701.
- (24) Casalini, R.; Roland, C. M. *J. Chem. Phys.* **2009**, *131*, 114501.
- (25) Casalini, R.; Roland, C. M. *J. Non-Cryst. Solids* **2011**, *357*, 282–285.
- (26) Dhinojwala, A.; Wong, G. K.; Torkelson, J. M. *J. Chem. Phys.* **1994**, *100*, 6046.
- (27) Wojnarowska, Z.; Roland, C. M.; Kolodziejczyk, K.; Swiety-Pospiech, A.; Grzybowska, K.; Paluch, M. *J. Phys. Chem. Lett.* **2012**, *3*, 1238–1241.
- (28) Bohmer, R.; Ngai, K. L.; Angell, C. A.; Plazek, D. J. *J. Chem. Phys.* **1993**, *99*, 4201.
- (29) Adam, G.; Gibbs, J. H. *J. Chem. Phys.* **1965**, *28*, 139.
- (30) Avramov, I. J. *Non-Cryst. Solids* **2000**, *262*, 258; *J. Non-Cryst. Solids* **1998**, *238*, 6.
- (31) Paluch, M.; Roland, C. M. *J. Non-Cryst. Solids* **2003**, *316*, 413–417.
- (32) Casalini, R.; Mohanty, U.; Roland, C. M. *J. Chem. Phys.* **2006**, *125*, 014505.
- (33) Ngai, K. L.; Roland, C. M. *Macromolecules* **1993**, *26*, 6824.
- (34) Johari, G. P.; Power, G.; Vij, J. K. *J. Chem. Phys.* **2002**, *116*, 5908.
- (35) Kudlik, A.; Benkhof, S.; Blochowicz, T.; Tschirwitz, C.; Rössler, E. *J. Mol. Struct.* **1999**, *479*, 210.
- (36) Ngai, K. L.; Capaccioli, S. *Phys. Rev. E* **2004**, *69*, 031501.
- (37) Weyer, S.; Hensel, A.; Schick, C. *Thermochim. Acta* **1997**, *304/305*, 267–275.
- (38) Applications to Polymers and Plastics; Cheng, S. Z. D., Ed.; *Handbook of Thermal Analysis and Calorimetry*; Elsevier Science: Amsterdam, 2002; Vol. 3.

- (39) Fragiadakis, D.; Casalini, R.; Bogoslovov, R. B.; Robertson, C. G.; Roland, C. M. *Macromolecules* **2011**, *44*, 1149–1155.
- (40) Donth, E. *J. Non-Cryst. Solids* **1982**, *53*, 325.
- (41) Berthier, L.; Biroli, G.; Bouchaud, J. P.; Cipelletti, L.; El Masri, D.; L'Hote, D.; Ladieu, F.; Pierno, M. *Science* **2005**, *310*, 1797–1800.
- (42) Berthier, L.; Biroli, G.; Bouchaud, J. P.; Kob, W.; Miyazaki, K.; Reichman, D. R. *J. Chem. Phys.* **2007**, *126*, 184503.
- (43) Capaccioli, S.; Ruocco, G.; Zamponi, F. *J. Phys. Chem. B* **2008**, *112*, 10652–10658.
- (44) Casalini, R.; Fragiadakis, D.; Roland, C. M. *Macromolecules* **2011**, *44*, 6928–6934.